Analytical modal analysis of bent slot waveguides

Kirankumar R. Hiremath
Department of Mathematics,
Institute for Scientific Computing and Mathematical Modeling,
University of Karlsruhe,
Engesserstrasse 6, Geb. 20.52 76128, Karlsruhe, Germany
hiremath@math.uni-karlsruhe.de

(Published in J. of Optical Society of America A, vol 26 (11), p. 2321-2326, 2009)

Abstract

In this work we analyze modal properties of dielectric optical bent slot waveguides by using the multilayer formulation of the well known classical analytical model of bent waveguides based on the Bessel/Hankel functions. Unlike the previously studied approximate model based on the Airy functions, this model is valid for all values of bend radii. The present approach allows quick and accuracy computations of propagation constants, mode profiles, and field/power densities for the 2D bent slot waveguides with very small radii. Using this model we characterize the optimal slot position inside the bent core to maximize the field enhancement in the slot. Such modal analysis is quite useful for the design of devices involving bent slot waveguides. Moreover the results obtained by the present 2D rigorous analytical model can be also used for benchmarking other numerical tools.

1 Introduction

Guiding and confining light in low index nanometric slots offers novel opportunities like highly sensitive optical sensors, improved light-matter interaction for nonlinear optics applications, etc [1, 2, 3, 4]. Waveguiding in such structures provides high electric field density and high optical power density in the narrow slots which is not possible in the conventional waveguides.

Slot waveguides with bends are one of the important realizations of this configuration. Often these waveguides are simulated with finite difference methods [2, 3]. While using such methods, accurate resolution of the nanometric slot and the waveguide bending can become cumbersome. In Ref. [5] the bent slot waveguides are analyzed using analytical approximation with the Airy functions. This formulation is based on representing the 2D bent slot waveguide fields in terms of the Airy functions under the assumption that the bend radius of the waveguide is much larger than the waveguide width [6]. This approximation is a severe constraint for integrated optics applications involving very small bends. As we shall show later on, using the Airy functions approach in such cases will lead to erroneous estimations of the bend losses.

One can overcome these limitations by employing the classical frequency domain analytical model of the bent waveguides [7, 8]. While in the literature mostly its three layer configurations are analyzed, in this work we use its multilayer version. Perturbation method based on continuation of wave functions also has been used to analyze multilayer/multi-clad bent slab waveguides [9]; but it more applicable for a special case of W-type (doubly clad) bent slab waveguides. Although the complete analytical arguments as the classical model are possible only in 2D [10, 11], this approach has been successfully augmented and adapted to full 3D bent waveguides by means of semi-vectorial method of lines [12], vectorial method of lines [13], and field mode matching [14, 15]. These 3D bent waveguide models essentially differ in the way they treat the vertical direction, but all the methods share the common feature that the lateral (i.e. radial) direction is treated analytically with the Bessel/Hankel functions, as in case of the 2D classical model. Therefore without loss of the generality in this paper we focus on the 2D model, and explore its multilayer extension to analyze the modal properties of the bent slot waveguides.

One can get such 2D setting under appropriate conditions by using the effective index method (EIM) for 3D bent slot waveguides [5, 6]. Note that the applicability of this simplification crucially depends on the geometry of the 3D bent waveguide cross section, and the refractive index profile itself [12, 16].

The EIM is not applicable when the outer interface of the rib waveguide is below cutoff. Also improper application of the EIM artificially increases the refractive index contrast, resulting in incorrect estimation of bend losses.

Considering the formulation along the radial direction, the present 2D approach is similar to the 3D film mode matching method [14, 15]. The latter method uses the Hertz potentials along with the immittance matrix formulation, whereas the present method is directly formulated in terms of the electric and magnetic fields, and solved for the amplitudes of these fields (here we did not experience any numerical difficulties). As a special case with no field/permittivity variations in the vertical direction, one can simulate the 2D setting with the 3D film mode matching model. Indeed, in case of the 2D settings these two approaches are equivalent, but the present formulation is more intuitive, e.g. with this model the mode orthogonality, normalization, modal power can be analytically formulated and computed in terms of field amplitudes [11].

The solution method of the 2D analytical model is analogous to the Airy functions method in Refs. [5, 6], except that one does not make any assumption for validity of the solution, and does not make variable transformation. But the consequence is that then one has to compute the Bessel/Hankel functions with complex valued order (and possibly for large orders and arguments). Efficient routines for these computations are not easily available. The former method avoids this numerical obstacle by using the Airy functions method. We overcame this obstacle by using our in house implemented routines for the required Bessel/Hankel functions [11] based on the uniform asymptotic expansions of the Bessel functions [17] with the help of routines in Ref. [18]. This implementation is quite robust and fast. In subsequent text we discuss the results obtained with this Bessel/Hankel functions based approach.

2 Analytical model of bent slot waveguides

A typical 2D bent slot waveguide investigated here is shown in Fig. 1. As mentioned earlier, under appropriate conditions one can get such 2D setting by using the EIM for 3D bent slot waveguides. The quasi transverse electric (TE) mode in 3D slot waveguides has the principal magnetic field component in the y direction, which is equivalent to the (pure) transverse magnetic mode (TM) in the present setting. Similar relationship holds for the quasi TM mode and the (pure) TE mode. We model the 2D bent slot waveguide as a multilayer planar bent waveguide. This is an extension of the well studied 3 layer planar bent waveguides, for which we have pure analytical model [7, 8] with reliable numerical implementation [11]. As mentioned earlier, this 2D multilayer formulation is similar to the radial representation in the 3D film mode matching method [14] or the method of lines [16].

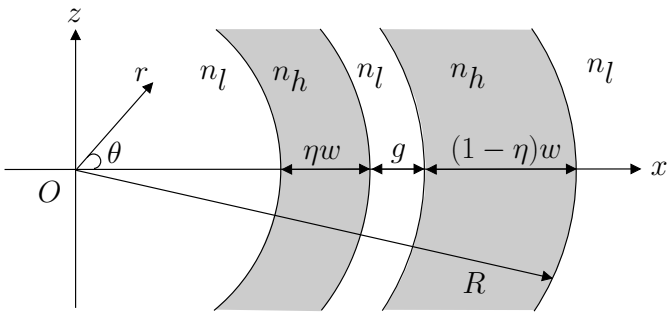

Figure 1: Bent slot waveguide: A slot of low refractive index n_l and width g is formed in between two regions of high refractive index n_h and widths ηw and $(1-\eta)w$ resp., where w is the total width of the regions with the high refractive index, and $0 \leq \eta \leq 1$ is the asymmetry parameter ($\eta = 0.5$ corresponds to the symmetrical waveguide setting). The total width of the waveguide core is $w_{tot} = w + g$. The bend radius R is defined as the outermost material interface of the core.

Consider a bent slot slab waveguide with the y-axis as the axis of symmetry as shown in Fig. 1. Assume that the material properties and the fields do not vary in the y-direction. Being specified by radial dependent piecewise constant refractive index $n(r)$, the waveguide can be seen as a homogeneous structure along the angular coordinate θ. Hence we choose an ansatz for the bent modes with pure exponential dependence on the azimuthal angle θ, where the angular mode number is written as a product γR with a reasonably defined bend radius R, such that γ can be interpreted as the propagation

constant. Here we define the bend radius R as in Fig. 1. For different choices of R, and their consequences, see Sec. 3.

In the cylindrical coordinate system (r, y, θ), the propagating electric field $\vec{E}$ and the magnetic field $\vec{H}$ (in the usual complex notation) are given by

$$\begin{pmatrix}\vec{E}\\ \vec{H}\end{pmatrix}(r,\theta,t) = \begin{pmatrix}(\tilde{E}_r, \tilde{E}_y, \tilde{E}_\theta)\\ (\tilde{H}_r, \tilde{H}_y, \tilde{H}_\theta)\end{pmatrix}(r)\ \exp\left(i(\omega t - \gamma R\theta)\right), \tag{1}$$

where the $\sim$ symbol indicates the mode profile, γ is the propagation constant of the bend mode, and $\omega = 2\pi c/\lambda$ is the angular frequency corresponding to the given vacuum wavelength λ, c is the speed of light in vacuum. Since the optical field propagating in the bent waveguide losses energy due to bending of the waveguide, γ is complex valued, expressed as $\gamma = \beta - i\alpha$, where β and α are real valued the phase propagation constant and the attenuation constant resp..

Inserting the ansatz (1) into the Maxwell curl equations, one obtains two decoupled sets of equations [11]: One set for the TE waves for which the nonzero components are $\tilde{E}_y$, $\tilde{H}_r$ and $\tilde{H}_\theta$, which are expressed in terms of $\tilde{E}_y$; and the second set for the TM waves with the nonzero components are $\tilde{H}_y$, $\tilde{E}_r$ and $\tilde{E}_\theta$, which are given in terms of $\tilde{H}_y$.

Within the radial intervals with the constant refractive index n, the principal component $\phi = \tilde{E}_y$ (TE) or $\phi = \tilde{H}_y$ (TM) satisfies the Bessel equation $\frac{d^2\phi}{dr^2} + \frac{1}{r}\frac{d\phi}{dr} + (n^2k^2 - \frac{\gamma^2R^2}{r^2})\phi = 0$ with complex order γR, where $k = 2\pi/\lambda$ is the given, real valued vacuum wavenumber. In the core regions the solution is represented as a linear combination of the Bessel function of the first kind J, and the second kind Y. For bounded solution at the origin, the solution in the interior is expressed in terms of the Bessel function of the first kind J, whereas for the outgoing wave solution as $r \to \infty$, we expressed the solution in the exterior in terms of the Hankel function of the second kind $\mathrm{H}^{(2)}$ [11]. Thus for the present single slot structure, the general solution for $\phi(r)$ in the various regions is given by

$$\phi(r) = \begin{cases} A_0\mathrm{J}_{\gamma R}(n_l kr), & \text{if } \ 0 \le r \le R-w-g,\\ A_1\mathrm{J}_{\gamma R}(n_h kr) + B_1\mathrm{Y}_{\gamma R}(n_h kr), & \text{if } \ R-w-g \le r \le R-(1-\eta)w-g,\\ A_2\mathrm{J}_{\gamma R}(n_l kr) + B_2\mathrm{Y}_{\gamma R}(n_l kr), & \text{if } \ R-(1-\eta)w-g \le r \le R-(1-\eta)w,\\ A_3\mathrm{J}_{\gamma R}(n_h kr) + B_3\mathrm{Y}_{\gamma R}(n_h kr), & \text{if } \ R-(1-\eta)w \le r \le R,\\ A_4\mathrm{H}^{(2)}_{\gamma R}(n_l kr), & \text{for } \ r \ge R, \end{cases} \tag{2}$$

where A_i, B_i for $i = 0$ to 4 are a priori unknown constants. This procedure can be easily generalized to multi-slot setting by taking into account corresponding linear combinations of the Bessel functions J and Y for the fields in the inner layers.

For the TM fields the material interface conditions require (i) continuity of the tangential component of the magnetic field $\tilde{H}_y$, (ii) continuity the tangential component of the electric field $\tilde{E}_\theta$, which is equivalent to continuity of $\frac{1}{n^2}\frac{\partial \tilde{H}_y}{\partial r}$, and (iii) continuity the normal component of the electric displacement field $n^2\tilde{E}_r$, which is equivalent to continuity $\tilde{H}_y$. As a direct consequence of the third condition, the normal component of the electric field $\tilde{E}_r$ is discontinuous at the material interfaces, and it is high in the low index slot (see Fig. 2 for illustrations.). Thus for nanometric slot widths, this TM configuration allows subwavelength confinement of light in the slot [1]. In the subsequent discussions, we restrict ourselves for the TM setting.

The first two interface conditions are used to determine the unknowns A_i and B_i (Note that enforcing the condition (i) is equivalent to enforcing the condition (iii)). This leads to a homogenous system of linear equations for A_i and B_i. Due to sparsity of the matrix involved, evaluation of the determinant by the row expansion is feasible. For a given frequency ω, for a nontrivial solution the determinant of this system must be singular, which leads to the dispersion equation in terms of γR for the bent slot waveguides. This equation is solved for the propagation constants γ.

It involves searching for complex valued roots, and need to compute the Bessel/Hankel functions with complex valued order. The former is done with the secant method, while the latter one is accomplished by using the uniform asymptotic expansions of the Bessel functions [17]. The modes are labeled by the number of minima for the absolute value of the principal component in the high index core regions. As in Ref. [11], it can be also shown that the bend modes satisfy relevant orthogonality condition, and can be power normalized.

3 Comparison

Having discussed the theoretical aspects of the modeling, now we present simulation results. For comparison, we take the test case in Ref. [5]: A bent slot waveguide with $n_h = 2.914406$, $n_l = 1$, $w = 0.4\,\mu$m, $g = 50$ nm, $\eta = 0.5$, $\lambda = 1.55\,\mu$m. For various bent radii R, the TM modes of this structure are computed. The results are compared with those of obtained with the Airy functions approach [5, 6]. The accuracy of the implementation of the Airy functions approach used here is validated against the reference data in [6], and an excellent agreement has been found.

Observe the notation differences between the setting in Ref. [5] and the current setting: (i) In the reference setting, the harmonic time dependence for the field ansatz is $\exp(-i\omega t)$, and the real and imaginary part of the propagation constant are positive. By the time reversal and space reversal properties of the Maxwell equations [19], this is equivalent to the present setting with the time dependence $\exp(i\omega t)$ and negative imaginary part of the propagation constant. (ii) In the reference setting, the bend radius $R_{\rm ref}$ is defined as the distance between the origin and the center of the waveguide core. The resultant values of the propagation constants $\gamma_{\rm ref}$ differ from the corresponding values γ in the present work. Nevertheless, one must expect $\gamma_{\rm ref} R_{\rm ref} = \gamma R$ [11]. Here we follow the definition of the bend radius R as depicted in Fig. 1.

Table 1 shows the comparison for the effective index $N_{\rm eff} = \gamma/k$. While the current analytical model is valid for all values of the bend radius R, as mentioned earlier the Airy functions model is applicable when R is much larger than the width of the waveguide core $w_{\rm tot}$ [6]. In the present setting, for larger bent radii like $R = 25\,\mu$m, $20\,\mu$m the results are reasonably agreeing with each other (due to large R, the attenuation constant is practically zero). But as R decreases, the discrepancy starts to appear. It is found that for the smaller bent radii the Airy functions approach overestimates the values of real and imaginary part of $N_{\rm eff}$ (or of the propagation constants). Thus the present model is better suited to analyze the functioning of slot devices involving bent waveguides with small radius.

Radius	Present method		Airy functions method [5]	
R μm	Re($N_{\rm eff}$)	|Im($N_{\rm eff}$)|	Re($N_{\rm eff}$)	Im($N_{\rm eff}$)
25.0	1.65668	(≈ 0)	1.65690	(≈ 0)
20.0	1.65295	(≈ 0)	1.65329	(≈ 0)
10.0	1.63440	(≈ 0)	1.63572	5.18310×10^{-11}
9.0	1.63030	(≈ 0)	1.63193	5.30060×10^{-10}
7.0	1.61864	6.35039×10^{-13}	1.62132	5.54679×10^{-8}
5.0	1.59784	2.18401×10^{-9}	1.60310	5.81667×10^{-6}
2.5	1.52746	5.68646×10^{-5}	1.54939	2.01261×10^{-3}

Table 1: Comparison of simulation results for the effective index $N_{\rm eff} = \gamma/k$ of $\rm TM_0$ mode of the slot waveguide in Section 3. '≈ 0' means that the corresponding value is numerically equivalent to zero. Also see the remarks in Sec. 3 about the notation differences in the two methods.

4 Effect of inclusion of slot

Recently microresonators with the cavity made up of slot waveguide have been demonstrated for novel sensing applications [20]. Such configurations complement the usual resonance properties (e.g. resonance field enhancement, high interaction length with small device footprint) with the unique feature of waveguiding in the low index cavity slot. When modeling these resonators in frame work of the coupled mode theory [21], the bent slot waveguides come into the picture. As the slot in the cavity waveguide influences the bending/cavity loss, which in turn influences the Q of the resonator, from device design point of view one is interested in effect of the slot inclusion. As a step towards such understanding, we begin further analysis by investigating the effect of introducing a slot in the conventional three layer bent waveguide (slot width $g = 0$).

The slot is introduced in the center of the waveguide core i.e. the asymmetry parameter $\eta = 0.5$. As shown in Fig. 2(first column), the waveguide without slot is monomodal; supporting a moderately lossy $\rm TM_0$ mode, which is reasonably well confined to the core. These modal fields show typical field displacement (towards outer material interface $r = R = 0$) associated with the bent waveguides. Presence of the slot markedly changes the nature of the modal solutions. A single hump of the principal component $\tilde{H}_y$ of the three layer waveguide gets split into two parts each confined to the associated high index region

(see first row). It is accompanied by the high field strength of the electric field component $\tilde{E}_r$ in the low index slot region (see second row). Further increasing the slot width decreases the electric field enhancement in the slot.

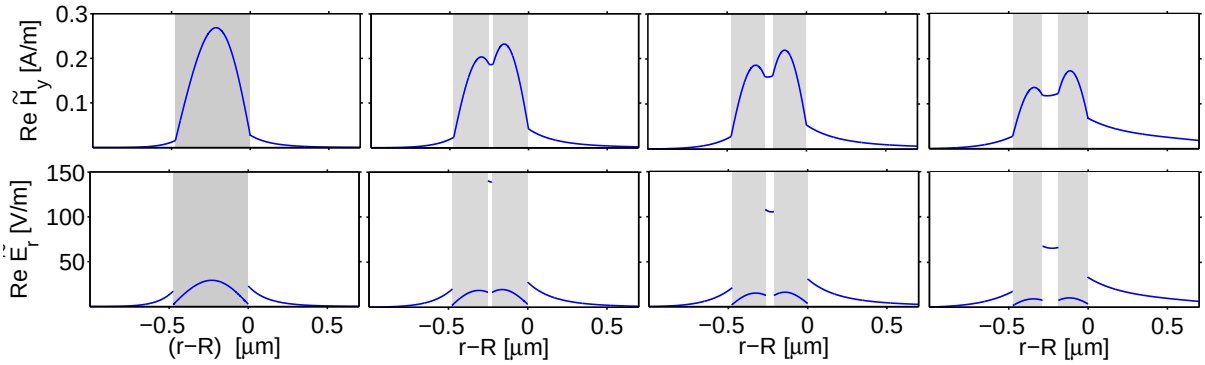

Figure 2: Effect of inclusion of the slot on modal solutions $\tilde{H}_y$ (first row) and $\tilde{E}_r$ (second row). A slot of width 25 nm (second column), 50 nm (third column), and 100 nm (forth column) was introduced in a 3 layer bent waveguide (first column) made up of a core of refractive index $n_h = 2.914406$ and width $w_{\text{tot}} = 0.475\,\mu$m, embedded in the surrounding medium of refractive index $n_l = 1$, $R = 2\,\mu$m, $\lambda = 1.55\,\mu$m, and the slot position given by $\eta = 0.5$. N_{eff} of the modes are given in Table 2. The field profiles are power normalized.

The influence of the slot width on the effective index of TM_0 is as shown in Table 2. The perturbation by the low index slot disturbs the confinement in the waveguide core causing decrease in the real part of the effective index, and increase in the imaginary part of the effective index. This effect is stronger for small bend radius, and large slot width.

g nm	N_{eff} for $R = 2\,\mu$m	N_{eff} for $R = 3\,\mu$m
0	$2.18110 - i\,2.77771 \times 10^{-10}$	$2.27597 - i\,1.07239 \times 10^{-15}$
25	$1.74970 - i\,3.94677 \times 10^{-6}$	$1.82393 - i\,3.40851 \times 10^{-9}$
40	$1.61391 - i\,5.33288 \times 10^{-5}$	$1.68078 - i\,2.26709 \times 10^{-7}$
50	$1.54201 - i\,1.91639 \times 10^{-4}$	$1.60449 - i\,1.81824 \times 10^{-6}$
75	$1.40191 - i\,1.84535 \times 10^{-3}$	$1.45373 - i\,7.72307 \times 10^{-5}$
100	$1.29990 - i\,7.75907 \times 10^{-3}$	$1.34169 - i\,8.68818 \times 10^{-4}$

Table 2: Effect of the slot width g on the effective index. The bent slot waveguide configuration is same as that of for Fig. 2.

For a fixed slot width g, the effect of bend radius on the symmetric bent slot waveguide is shown in Fig. 3. As the bend radius increases, the real part of N_{eff} of the bent mode tends to that of equivalent straight slot waveguide (with $N_{\text{eff}} = 1.8213945, 1.7378974, 1.665327$ for $g = 40, 50, 60$ nm resp.). The attenuation constant (in terms of imaginary part of N_{eff}) shows the characteristic exponential dependence on R. This behavior ensures the reliability of the numerical results even for small bent radii.

5 Effect of position of the slot

So far we considered the settings where the slot is symmetrically positioned in the center of the total waveguide core (i.e. $\eta = 0.5$). The position of the slot also affects the modal solutions of the slot waveguides. Variation of the effective index for different values of η is systematically shown in Fig. 4. It is found that the real part and the imaginary part of N_{eff} do not attain their extremum at the symmetric position $\eta = 0.5$. This observation is consistent with the Ref. [2].

This asymmetry is the consequence the field displacement in the bent waveguides. As shown in Fig. 5 (first column), in the "unperturbed" (i.e. without slot) bent waveguide the field is localized slightly closer to outer interface $r - R = 0$. Due to the bending, the peak for $\tilde{H}_y$ (which is at $r - R = -0.2367$) is shifted away from the center of the core (which is $r - R = -0.2375$) towards the outer radial interface. When the slot is positioned in the vicinity of the field peak, the resultant perturbation is significant, which is reflected in smaller values of $\text{Re}(N_{\text{eff}})$ and higher $\text{Im}(N_{\text{eff}})$ in Fig.4.

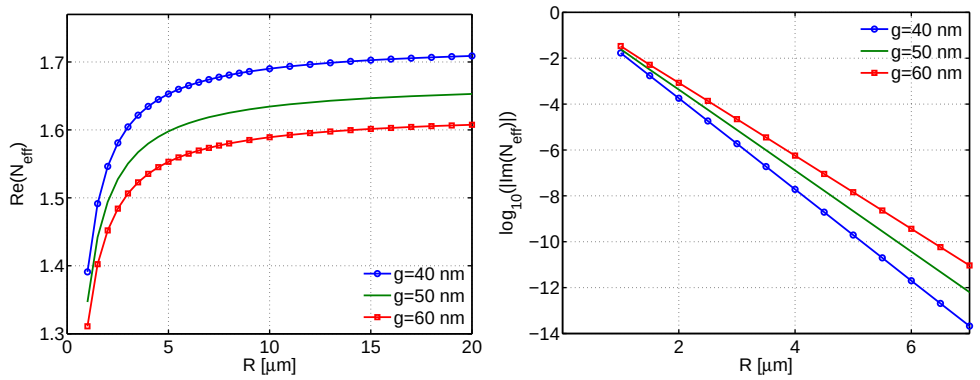

Figure 3: Effect of the bend radius on the effective index of bent slot waveguide. The bent slot waveguide configuration is same as that of for Fig. 2.

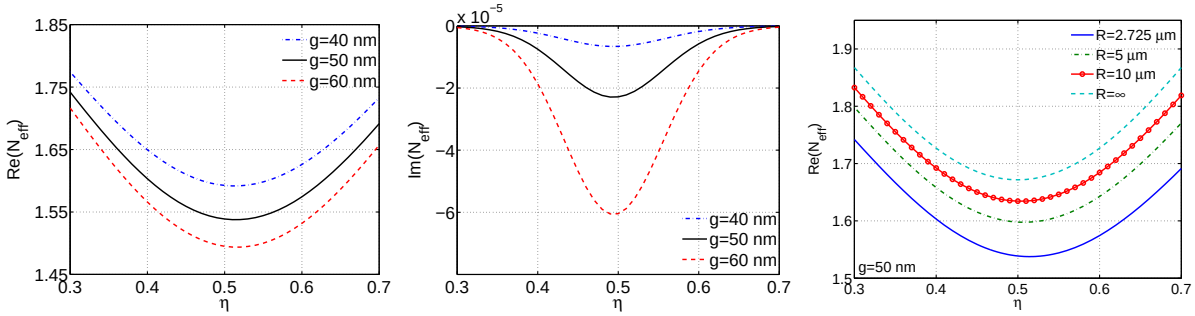

Figure 4: Effect of the slot position on the real part (left) and and the imaginary part (center) of the effective index of the bent slot waveguide with $R = 2.725\,\mu$m. $n_h = 2.914406$, $n_l = 1$, w=0.4 μm, $\lambda = 1.55\,\mu$m. For a fixed slot width $g = 50$ nm, the right most plot shows influence of the bend radius of the symmetry of the curves of real part of N_{eff} . $R = \infty$ corresponds to the straight waveguide.

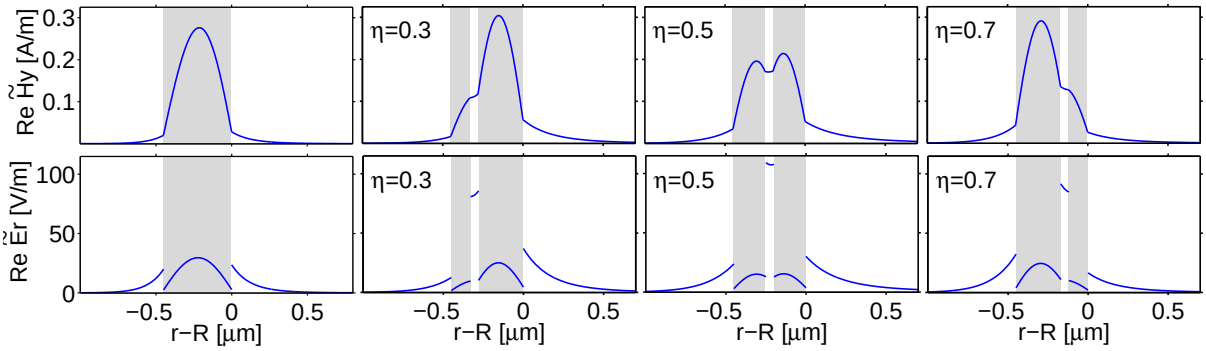

Figure 5: Effect of position of the slot. From left to right, the plots show the modal solution for $\tilde{H}_y$ (first row) and for $\tilde{E}_r$ (second row) with no slot, with slot positioned with $\eta = 0.3, 0.5, 0.7$ resp.. The effective index for these modal solutions are $2.25671 - i\ 2.81308 \times 10^{-14}$, $1.74200 - i\ 2.64315 \times 10^{-7}$, $1.53877 - i\,2.28484 \times 10^{-5}$, $1.69136 - i\,1.90260 \times 10^{-7}$ resp.. The waveguide configuration is $n_h = 2.914406$, $n_l = 1$, $w_{\text{tot}} = 0.45\,\mu$m, $g = 50$ nm, $R = 2.725$, $\lambda = 1.55\,\mu$m.

The above bent field displacement is smaller for larger bend radii. Therefore for bent slot waveguides with large radii, minimum of the real part of N_{eff} attains closer to $\eta = 0.5$ as shown in Fig. 4. For comparison, when $R = \infty$, i.e. for a straight slot waveguide, the minimum is exactly at $\eta = 0.5$.

Plots in Fig. 5 show this effect on the field distribution of the principal component $\tilde{H}_y$ and the dominant component $\tilde{E}_r$. It is found that when the perturbation as a function of η is maximum, the field concentration of the dominant component in the slot is also maximum. This insight is used in the next section to optimize the slot position for maximum field enhancement in the slot.

6 Optimizing the slot position

From applications point of view, one is interested in high power concentration in the slot. Fig. 6(left) shows variation of the normalized power in the slot for various slot positions. As seen in this plot, there is a certain range of η for which there is more power in the low index slot (dash line) compared to high index core layers on the left and right side of the slot. For the setting under consideration, for $\eta = 0.52$ the power in the slot attains maximum (=46.23%). One is also interested in the slot power density, which is defined as the power in the slot divided by the slot width. Fig. 6(right) shows the variation of the slot power density for different slot positions. The power density in the slot is maximum when the slot is positioned in the region of field maximum for the corresponding unperturbed bent waveguide.

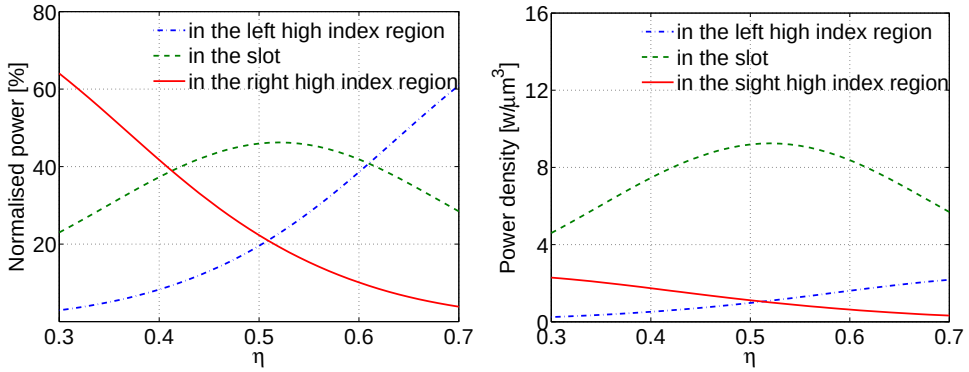

Figure 6: Effect of the slot position on the power in the slot (left) and the slot power density (right). Bent slot waveguide is as in Fig. 5.

7 Conclusions

In this paper we investigated the bent slot waveguides using the multilayer formulation of the analytical model of bent waveguides. We simulated effect of the slot width and the slot position on the TM modal solutions of the slot waveguides of various bend radii. It is shown that the influence of the slot is maximum when it is positioned in the region of field maximum of the TM mode principal component $\tilde{H}_y$ of the corresponding unperturbed (i.e. without slot) bent waveguide. In this case the electric field enhancement and the power density in the slot region are maximum. Unlike the approximate model based on the Airy functions, the present 2D analytical model is robust and reliable even for small bent radii and subwavelength slot widths. Using the effective index method –where it is applicable– along with the present analytical model, one can analyze 3D bent slot waveguides. The results derived from the analytical model discussed in this paper can be used for benchmarking other numerical tools.

Acknowledgment

This work is funded by the Deutsche Forschungsgemeinschaft (German Research Council) Research Training Group 'Analysis, Simulation and Design of Nanotechnological Processes', University of Karlsruhe. The author acknowledges fruitful discussions with Chung-Yen Chao and Andreas Rieder. He thanks Manfred Hammer for providing the straight waveguide mode solver.

References

[1] V. R. Almeida, Q. Xu, C. A. Barios, and M. Lipson, "Guiding and confining light in void nanostructure," Optics Letters **29**, 1209–1211 (2004).

[2] P. A. Anderson, B. S. Schmidt, and M. Lipson, "High confinement in silicon slot waveguides with sharp bends," Optics Express **14**, 9197–9202 (2006).

[3] N.-N. Feng, J. Michel, and L. C. Kimerling, "Optical field concentration in low-index waveguides," IEEE J. of Quantum Electronics **42**, 885–890 (2006).

[4] C. Koos, P. Vorreau, T. Vallaitis, P. Dumon, W. Bogaerts, R. Baets, B. Esembeson, I. Biaggio, T. Michinobu, F. Diederich, W. Freude, and J. Leuthold, "All-optical high-speed signal processing with silicon-organic hybrid slot waveguides," Nature Photonics **3**, 216–219 (2009).

[5] C.-Y. Chao, "Simple and effective calculation of modal properties of bent slot waveguides," J. of the Optical Society of America B **24**, 2373–2377 (2007).

[6] J. Lu, S. He, and V. G. Romanov, "A simple and effective method for calculating the bending loss and phase enhancement of a bent planar waveguide," Fiber and Integrated Optics **24**, 25–26 (2005).

[7] E. A. J. Marcatili, "Bends in optical dielectric guides," The Bell System Technical Journal **48**, 2103–2132 (1969).

[8] L. Lewin, D. C. Chang, and E. F. Kuester, *Electromagnetic Waves and Curved Structures* (Peter Peregrinus Ltd. (On behalf of IEE), Stevenage, England, 1977).

[9] S. Kawakami, M. Miyagi, and S. Nishida, "Bending losses of dielectric slab optical waveguide with double or multiple claddings: theory," Applied Optics **14**, 2588–2597 (1975).

[10] E. C. M. Pennings, "Bends in optical ridge waveguides, modelling and experiment," Ph.D. thesis, Delft University, The Netherlands (1990).

[11] K. R. Hiremath, M. Hammer, S. Stoffer, L. Prkna, and J. Čtyroký, "Analytic approach to dielectric optical bent slab waveguides," Optical and Quantum Electronics **37**, 37–61 (2005).

[12] J. S. Gu, P. A. Besse, and H. Melchior, "Method of lines for the analysis of the propagation characteristics of curved optical rib waveguides," IEEE J. of Quantum Electronics **27**, 531–537 (1991).

[13] W. Pascher and R. Pregla, "Vectorial analysis of bends in optical strip waveguides by the method of lines," Radio Science **28**, 1229–1233 (1993).

[14] L. Prkna, M. Hubálek, and J. Čtyroký, "Vectorial eigenmode solver for bent waveguides based on mode matching," IEEE Photonics Technology Letters **16**, 2057–2059 (2004).

[15] L. Prkna, M. Hubálek, and J. Čtyroký, "Field modeling of circular microresonators by film mode matching," IEEE J. of Selected Topics in Quantum Electronics **11**, 217–223 (2005).

[16] W. Pascher, "Modelling of rib waveguide bends for sensor applications," Optical and Quantum Electronics **33**, 433–449 (2001).

[17] M. Abramowitz and I. A. Stegun, *Handbook of Mathematical Functions (Applied Mathematics Series 55)* (National Bureau of Standards, Washington, D.C., 1964).

[18] D. E. Amos, "A portable package for Bessel functions of a complex argument and nonnegative order," (1983). Http://www.netlib.org/amos/ .

[19] T. Tamir (editor), *Integrated Optics (Second Corrected and Updated Edition)*, vol. 7 of *Topics in Applied Physics* (Springer-Verlag, Germany, 1982).

[20] T. Baehr-Jones, M. Hochberg, C. Walker, and A. Scherer, "High-Q optical resonators in silicon-on-insulator-based slot waveguides," Applied Physics Letters **86**, 081101:1–3 (2005).

[21] K. R. Hiremath, R. Stoffer, and M. Hammer, "Modeling of circular integrated optical microresonators by 2-D frequency domain coupled mode theory," Optics Communications **257**, 277–297 (2006).